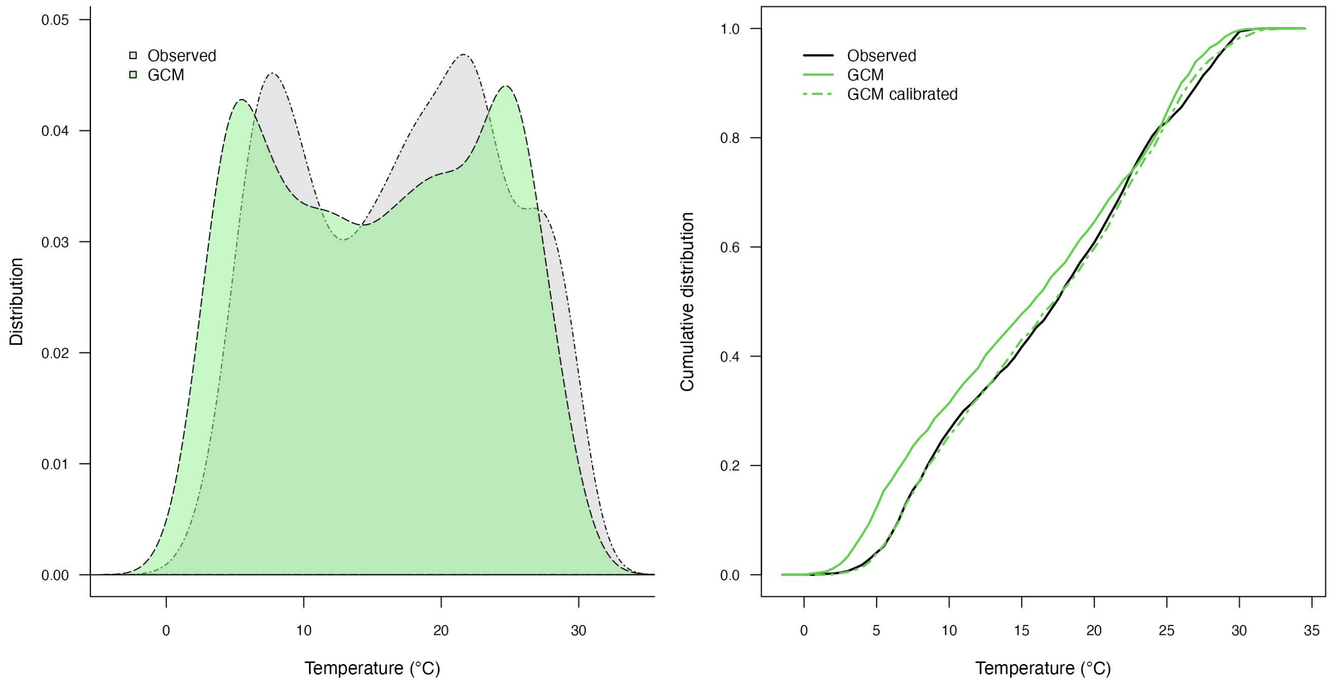

Supplementary Figure S1. Bias correction of the modeled temperature series in Kawasaki City, Japan. Distribution (left panel) and cumulative distribution (right panel) of the raw, bias-corrected modeled, and observed historical temperature series are compared.

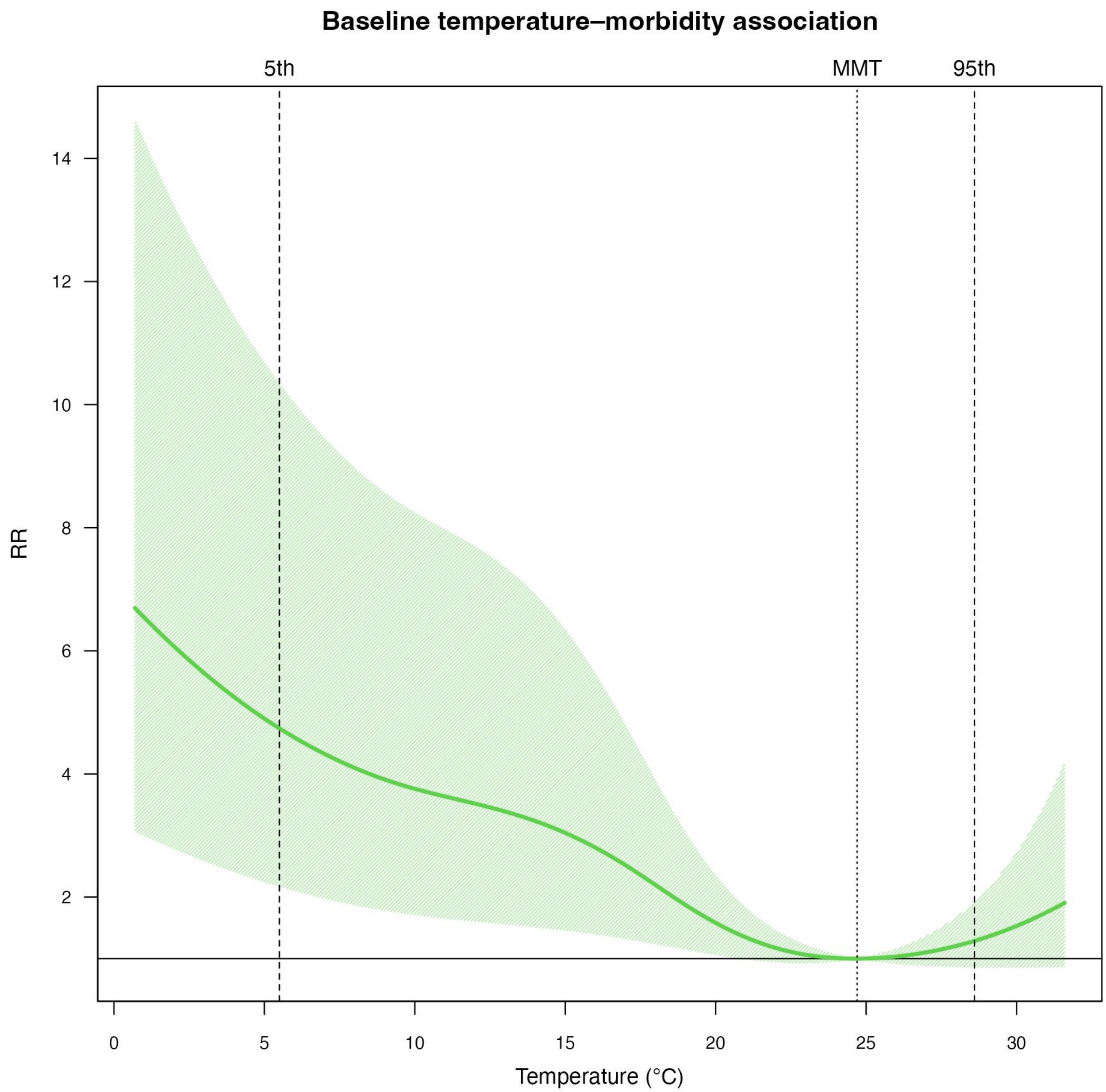

Supplementary Figure S2. Baseline overall cumulative association between temperature and influenza incidence across a lag of 0–14 days in Kawasaki City, Japan. The vertical dotted line corresponds to the minimum morbidity temperature (MMT), identified as 24.7°C at the 82^{nd} percentile. The vertical dashed lines represent the RRs calculated at the 5^{th} and 95^{th} percentiles. Abbreviations: MMT, minimum morbidity temperature; RR, relative risk.

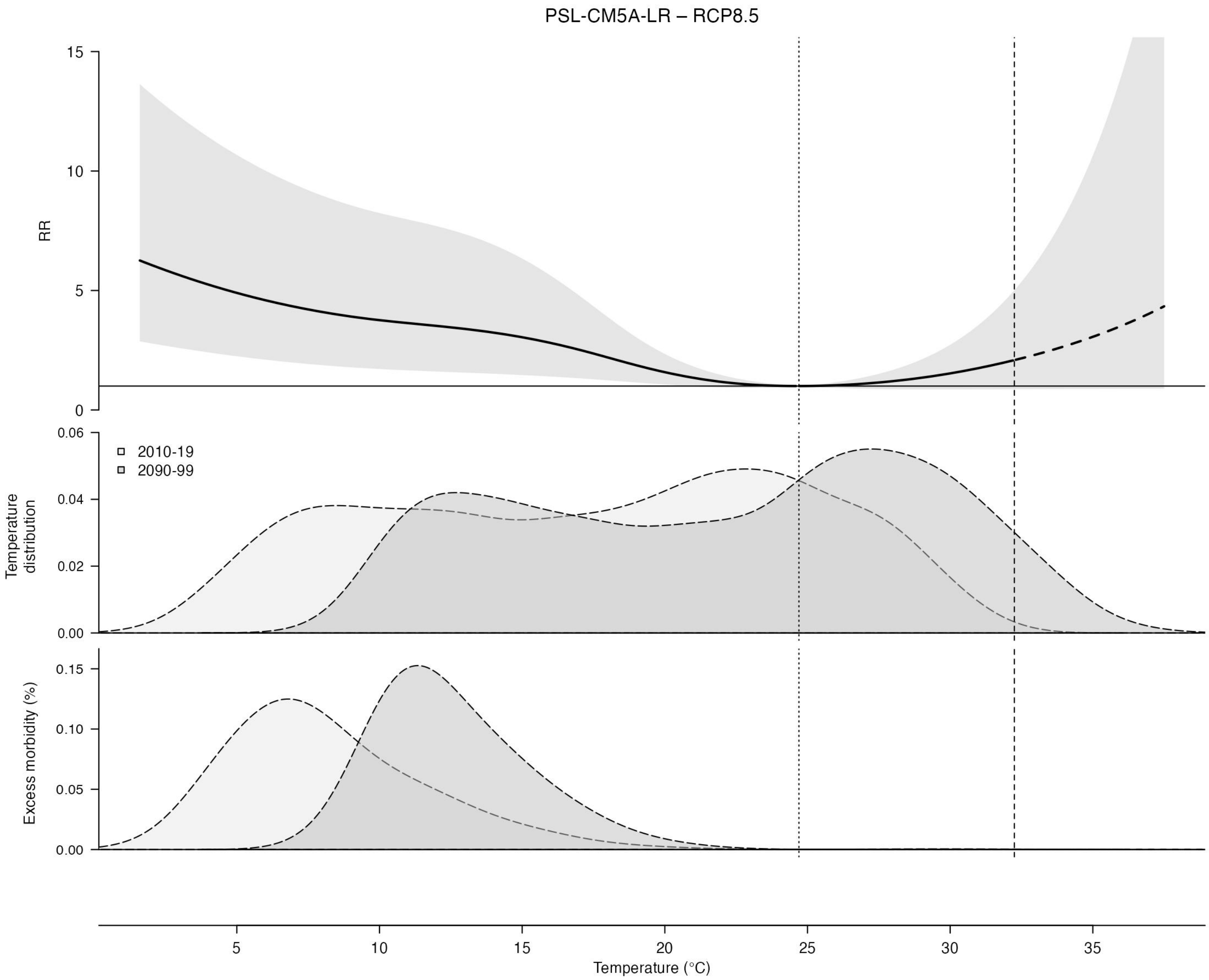

Supplementary Figure S3. Temperature and excess morbidity due to seasonal influenza in different climates in Kawasaki City, Japan. The top panel presents the estimated overall cumulative exposure–response relationships between relative risks (95% empirical confidence intervals) and the minimum morbidity temperature (MMT), used as a reference (dot). The curve highlights increased risks associated with cold and heat, with the dashed section extrapolating beyond the maximum temperature observed during 2010–2019 (dashed vertical line). The middle panel illustrates the distribution of modeled daily temperature series for the baseline period (2010–2019, light gray area) and projected future period (2090–2099, dark gray area), projected using a specific climate model (IPSL-CM5A-LR) and scenario (RCP8.5). The bottom panel shows the related distribution of excess morbidity in diarrhea, expressed as the excess seasonal influenza morbidity (%) related to non-optimal temperatures compared with MMT.

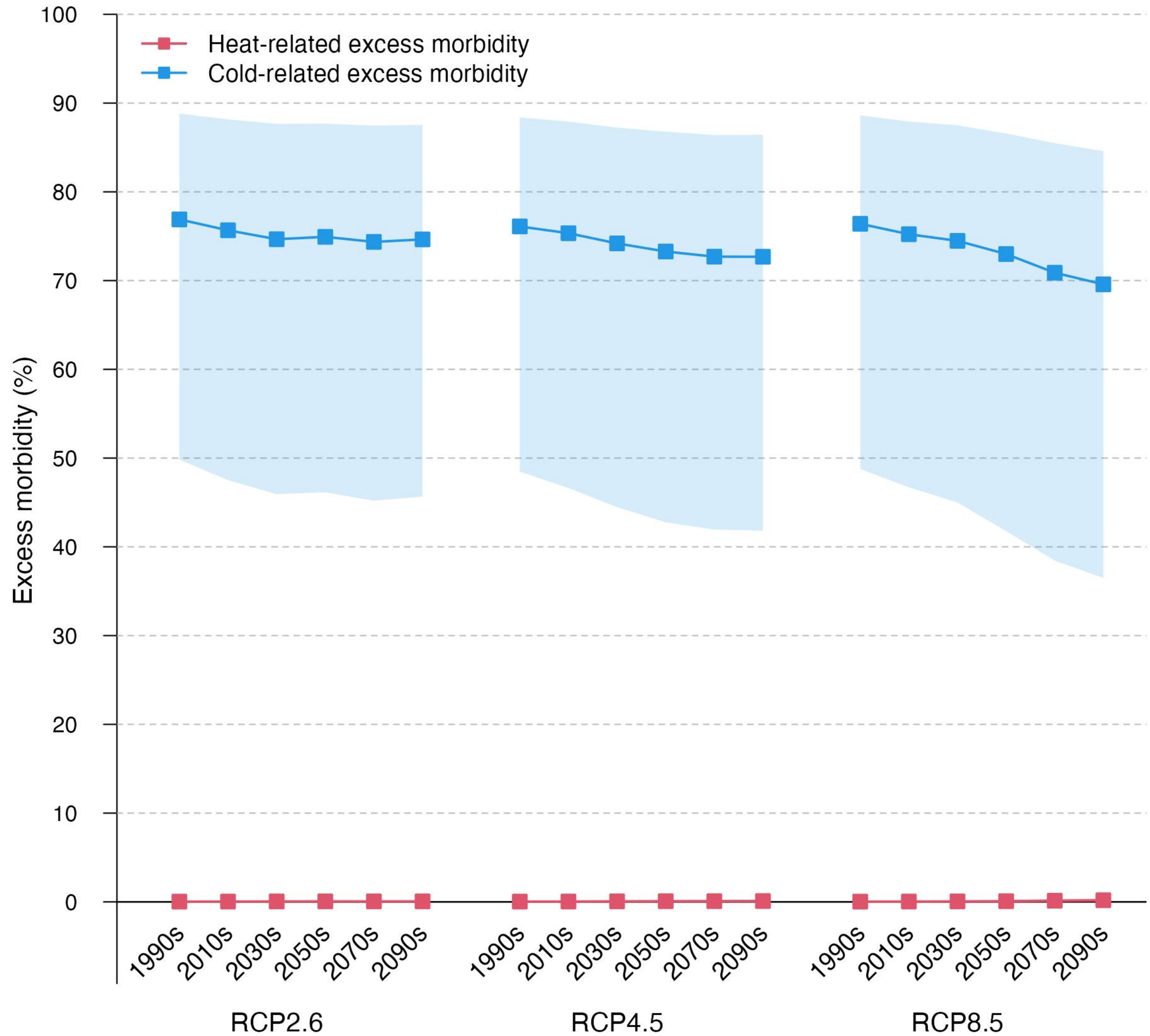

Supplementary Figure S4. Trends in heat- and cold-related excess morbidity due to seasonal influenza in Kawasaki City, Japan. The graph illustrates decadal excess morbidity attributed to heat and cold across three climate change scenarios: RCP2.6, RCP4.5, and RCP8.5. Estimates are expressed as GCM-ensemble mean decadal fractions—PSL-CM5A-LR, MIROC5, HadGEM2-ES, and GFDL-ESM2M—with shaded regions denoting 95% empirical confidence intervals.

Supplementary Table S1. Descriptive statistics of daily number of influenza cases, meteorological variables, and air pollutant concentrations

Variable	Number of cases	Mean	SD	Minimum	Maximum
Number of influenza (cases)	163,120	89.3	192.7	0	1,718
Mean temperature (℃)	–	16.8	7.5	0.7	31.6
Relative humidity (%)	–	68.4	15.8	28.0	99.0
Wind speed (m/s)	–	3.4	1.2	1.3	9.0
Total rainfall (mm)	–	4.8	14.3	0.0	192.5
Sunshine duration (hours)	–	5.7	4.2	0.0	13.8
$PM_{2.5}$ (μg/m^3)	–	11.2	5.6	0.7	40.1

Abbreviations: SD, standard deviation; $PM_{2.5}$, particulate matter <2.5 μm

Supplementary Table S2. Spearman's rank-order cross-correlation coefficients between daily number of influenza cases, meteorological variables, and air pollutant concentrations

Variable	1	2	3	4	5	6	7
1. Influenza	1.00						
2. Mean temperature	–0.82	1.00					
3. Relative humidity	–0.50	0.50	1.00				
4. Wind speed	0.11	–0.09	–0.14	1.00			
5. Total rainfall	–0.13	0.06	0.63	0.09	1.00		
6. Sunshine duration	0.03	0.09	–0.55	0.04	–0.59	1.00	
7. $PM_{2.5}$	–0.10	0.18	0.06	–0.27	–0.14	0.15	1.00

Abbreviations: $PM_{2.5}$, particulate matter <2.5 µm

Supplementary Table S3. Heat-related, cold-related, and net excess morbidity in influenza (%) with 95% empirical confidence interval by period under three climate change scenarios in Kawasaki City, Japan

Scenario	Effect	Period		
		2010–2019	2050–2059	2090–2099
RCP2.6	Heat	0.03 (−0.03, 0.08)	0.05 (−0.04, 0.12)	0.05 (−0.04, 0.12)
	Cold	75.66 (42.51, 88.16)	74.92 (46.14, 87.68)	74.64 (45.66, 87.54)
	Net	–	−0.71 (−2.02, 0.01)	−1.00 (−3.30, 0.04)
RCP4.5	Heat	0.03 (−0.03, 0.08)	0.07 (−0.06, 0.16)	0.09 (−0.06, 0.20)
	Cold	75.33 (46.62, 87.91)	73.27 (42.76, 86.78)	72.68 (41.82, 86.42)
	Net	–	−2.02 (−4.37, −0.95)	−2.59 (−5.95, 0.92)
RCP8.5	Heat	0.03 (−0.03, 0.08)	0.07 (−0.06, 0.17)	0.18 (−0.13, 0.41)
	Cold	75.22 (46.70, 87.91)	72.99 (41.77, 86.56)	69.57 (36.49, 84.58)
	Net	–	−2.19 (−5.15, −0.75)	−5.50 (−11.48, −1.72)

Notes: Data on projected temperature increases are the average mean prefecture-specific temperatures (range), as in the GM ensemble. Abbreviations: GCM, general circulation model; RCP, representative concentration pathway

Supplementary Table S4. Sensitivity analysis of the net difference in excess morbidity due to influenza in 2090–2099 compared with 2010–2019

Model	RCP2.6	RCP4.5	RCP8.5
	Net excess morbidity (%)	Net excess morbidity (%)	Net excess morbidity (%)
Main model	−1.00 (−3.30, 0.04)	−2.59 (−5.95, 0.92)	−5.50 (−11.48, −1.72)
Seasonal control: 5 df/year	−2.34 (−5.25, 0.17)	−5.68 (−9.49, −2.12)	−11.23 (−17.58, −3.82)
Position of knots: 10^{th}, 75^{th}, 90^{th} [a]	−1.65 (−5.93, 0.06)	−4.17 (−10.71, −1.30)	−8.71 (20.79, −2.53)
Maximum lag: 7 days	−0.89 (−2.44, 0.02)	−2.25 (−4.43, 0.86)	−4.60 (−8.41, −1.58)
Maximum lag: 21 days	−1.63 (−6.10, 0.00)	−4.05 (−11.27, −1.17)	−8.08 (−19.59, −2.32)
Adjustments: wind speed, total rainfall, sunshine duration, $PM_{2.5}$ [b]	−1.02 (−3.43, 0.04)	−2.64 (−6.15, −0.92)	−5.59 (−11.8, −1.74)

Notes: Results are the net difference in excess morbidity in 2090–2099 compared to 2010–2019. [a] Varying the positions of the knots in the cross-basis function from the 25^{th}, 50^{th}, and 75^{th} percentiles to the 10^{th}, 75^{th}, and 90^{th} percentiles. [b] Adjusted for 14-day moving average wind speed, sunshine duration, total rainfall, and $PM_{2.5}$ (modeled with a natural cubic spline with 3 df) as time-varying confounders. Abbreviations: df, degrees of freedom